Modelling of Conventional Swing of the Cricket Ball using Computational Fluid Dynamics

R M P S Bandara Head of the Department of Mechanical Engineering, N S Rathnayaka, Department of Information Technology & Mathematics, General Sir John Kotelawala Defence University

1. Introduction

Cricket is a sport that has the potential of attracting thousands of spectators to the stadiums around the world and also millions of people watch it on television through live coverage. In the Indian subcontinent especially, it has become a religion rather than a sport that brings the population together united as a single nation. Cricket has also become commercialized at present where transactions worth millions of dollars are taking place. However the beauty of this sport lies when the bowler and the batsman try to dominate each other for supremacy. This paper concentrates on one important aspect that enables bowlers to dominate the game over batsmen.

There exist two vital phases during the delivery of the cricket ball. During the first phase, the ball undergoes free flight from the point it is released from the bowler's hand until it hits the pitch. During this phase the motion of the ball is entirely under the influence of aerodynamic forces and the bowler is capable of controlling its motion to a considerable extent. The second phase involves the travel of the ball towards the batsman after bouncing off the pitch. During this phase the motion of the ball is basically governed by the orientation of the ball when it bounces off the pitch and the condition of the pitch and hence the bowler has less control on the ball. Although the bowlers try to dominate the proceedings through the control of the ball by exploiting the flight or flow conditions, it is doubtful whether they really understand the physical phenomena behind such endeavours.

The speed at which a bowler delivers the cricket ball can be categorized as fast bowling, where the speed is in the range from 130 to 150+ km/h, medium fast bowling in the range from 95 to 130 km/h and slow bowling, in the speed range from 70 to 95 km/h (Sayers & Lelimo 2007). Fast and medium fast bowlers in cricket use different strategies in their possession to defeat batsmen. Some of them are air swing, seam movement off the pitch, bouncer and yorker. Air swing of the cricket ball can be broadly categorized as conventional swing, reverse swing and contrast swing. Conventional swing takes place when the cricket ball is new, during the early stages of an innings of a cricket match, when the ball is delivered keeping the seam at an angle with the line of delivery. To assist the conventional swing, fast bowlers keep one side of the cricket ball shiny by polishing it on a regular basis and maintain the other side rough. During this phenomenon, deviation of the cricket ball takes place in the direction of the seam orientation, as it travels through the air. The primary seam which is playing a key role in conventional swing has been raised about 2 mm above the spherical surface of the ball. On either side of this primary seam and parallel to it around the surface there are two rows of 80 to 90 stitches that stand about 1 mm above the spherical surface (Sayers & Lelimo 2007).

Several attempts have been made to measure the aerodynamic forces acting on the cricket ball experimentally. Barton (1982) measured side forces on cricket balls by using a compound pendulum system where the ball was allowed to swing transversely. The side force was evaluated after the transverse deflection was measured. This was performed for different ball speeds and seam angles with the influence of backspin and wobbling. However his experiments contained weaknesses re-

lated to the means of suspension of the ball and the simplified mathematical analysis used. Detailed pressure distributions along the equator of a ball provided with pressure tappings were measured by Bentley et al. (1982). Mehta (1985) presented different fluid dynamics phenomena on the flow over cricket balls. He quantified important parameters for investigating the critical Reynolds number for transition from laminar to turbulent boundary layer. Sayers and Hill (1999) measured the drag, lift and side force on a cricket ball at different speeds. Influence of external conditions imposed on the cricket ball in terms of top spin and roughness was determined with respect to lateral forces. Sayers (2001) investigated the phenomenon of reverse swing through experiments by modelling the cricket ball as a sphere with three distinct rings representing the seam. The side force for varying seam angles and ball speeds were observed. Sherwin and Sproston (1982) mounted a cricket ball on a strain-gauge balance and measured the side force and drag force on it directly.

2. Governing Principles

Nomenclature

Roman

C_d	Drag coefficient	
C_l	Lift coefficient	
C_s	Side force coefficient	
D	Drag force (y direction)	N
d	Diameter of cricket ball	m
k	Turbulent kinetic energy	m^2s^{-2}
L	Lift force (z direction)	N
Re	Reynolds number	
S	Side force (x direction)	N
U	Delivery speed of ball	ms^{-1}

Greek

α	Seam angle from y axis	(degrees)
ε	Turbulent dissipation rate	m^2s^{-3}
μ	Absolute viscosity of free stream	Nsm^{-2}
ρ	Density of free stream	$kg\ m^{-3}$
σ	Prandtl number	

Figure 1 illustrates the different aerodynamic forces acting on the cricket ball during its flight. In general the resultant aerodynamic force on the ball can be resolved into three mutually perpendicular components, namely; Side force (S), Drag force (D) and Lift force (L) acting in the x, y and z directions respectively. The presence of the aforementioned component forces will depend upon the seam angle of the ball and any spin that may be applied on its delivery. The angle of seam (α) is taken with respect to the line of delivery (y-direction). In addition, the magnitude of the forces will depend on flow parameters, speed of delivery and the respective force coefficients.

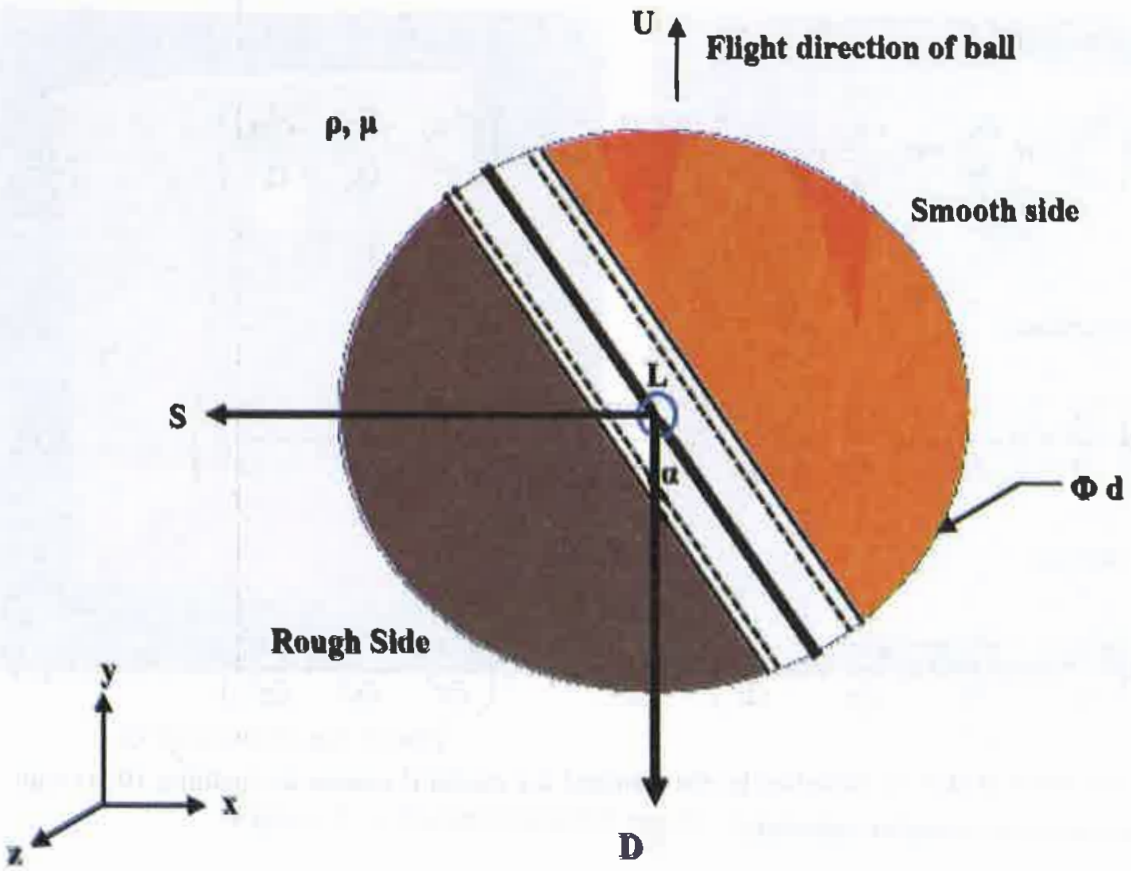

Figure 1: Aerodynamic forces on a cricket ball

Figure 1: Aerodynamic forces on a cricket ball

Drag force $$D = 0.5C_d\left(\frac{\rho\pi d^2U^2}{4}\right)$$ .....(1)

Lift force $$L = 0.5C_l\left(\frac{\rho\pi d^2U^2}{4}\right)$$ .....(2)

Side force $$S = 0.5C_s\left(\frac{\rho\pi d^2U^2}{4}\right)$$ .....(3)

Reynolds Number $$\mathrm{Re} = \frac{\rho Ud}{\mu}$$ .....(4)

The flow physics are governed by the Navier-Stokes equations as given below.

x direction

$$\rho\left(\frac{\partial u_x}{\partial t}+u_x\frac{\partial u_x}{\partial x}+u_y\frac{\partial u_x}{\partial y}+u_z\frac{\partial u_x}{\partial z}\right)=-\frac{\partial P}{\partial x}+\rho g_x+\mu\left(\frac{\partial^2 u_x}{\partial x^2}+\frac{\partial^2 u_x}{\partial y^2}+\frac{\partial^2 u_x}{\partial z^2}\right) \quad \text{..... (5)}$$

y direction

$$\rho\left(\frac{\partial u_y}{\partial t}+u_x\frac{\partial u_y}{\partial x}+u_y\frac{\partial u_y}{\partial y}+u_z\frac{\partial u_y}{\partial z}\right)=-\frac{\partial P}{\partial y}+\rho g_y+\mu\left(\frac{\partial^2 u_y}{\partial x^2}+\frac{\partial^2 u_y}{\partial y^2}+\frac{\partial^2 u_y}{\partial z^2}\right) \quad \text{.....(6)}$$

z direction

$$\rho\left(\frac{\partial u_z}{\partial t}+u_x\frac{\partial u_z}{\partial x}+u_y\frac{\partial u_z}{\partial y}+u_z\frac{\partial u_z}{\partial z}\right)=-\frac{\partial P}{\partial z}+\rho g_z+\mu\left(\frac{\partial^2 u_z}{\partial x^2}+\frac{\partial^2 u_z}{\partial y^2}+\frac{\partial^2 u_z}{\partial z^2}\right) \quad \text{.....(7)}$$

Turbulence of flow is modelled by the standard k-ε model (Launder & Spalding 1974) with the following transport equations:

$$\frac{\partial(\rho k)}{\partial t}+\nabla.(\rho k U)=\nabla.\left[\frac{\mu_t}{\sigma_k}\nabla k\right]+2\mu_t E_{ij}.E_{ij}-\rho\varepsilon \quad \text{..... (8)}$$

$$\frac{\partial(\rho\varepsilon)}{\partial t}+\nabla.(\rho\varepsilon U)=\nabla.\left[\frac{\mu_t}{\sigma_\varepsilon}\nabla\varepsilon\right]+C_{1\varepsilon}\frac{\varepsilon}{k}2\mu_t E_{ij}.E_{ij}-C_{2\varepsilon}\rho\frac{\varepsilon^2}{k} \quad \text{..... (9)}$$

where C_μ, σ_k, σ_ε, $C_{1\varepsilon}$ and $C_{2\varepsilon}$ are constants.

3. Methodology and Approach

With the availability of computers with higher processing speeds and scientifically validated CFD modelling tools, analyzing complex flow problems such as modelling of flow over the cricket ball has become possible with great accuracy. According to the law no. 5 imposed by the International Cricket Council, the mass of a new cricket ball should be from 0.156 kg to 0.163 kg and its diameter can vary between 71.3 mm and 72.9 mm. Hence the geometry of the cricket ball was modelled as a sphere of diameter 72 mm with the primary seam incorporated as a 20 mm wide concentric rim projecting 1 mm from the ball surface. Mass of the ball was taken as 0.160 kg. Figure 2 shows the 3-D computational model of the cricket ball generated by *GAMBIT 2.3.16*, a geometry modelling software having compatibility with the CFD tool and has shown high performance with complex geometry modelling. The computational field is represented by a rectangular parallelepiped domain having dimensions of 400 mm x 600 mm x 400 mm in the x, y and z directions respectively. The dimensions of the computational domain were determined such that the airflow over the cricket ball attains fully developed flow conditions. The ball was placed at a distance of 150 mm from the inlet boundary to capture the downstream effects effectively.

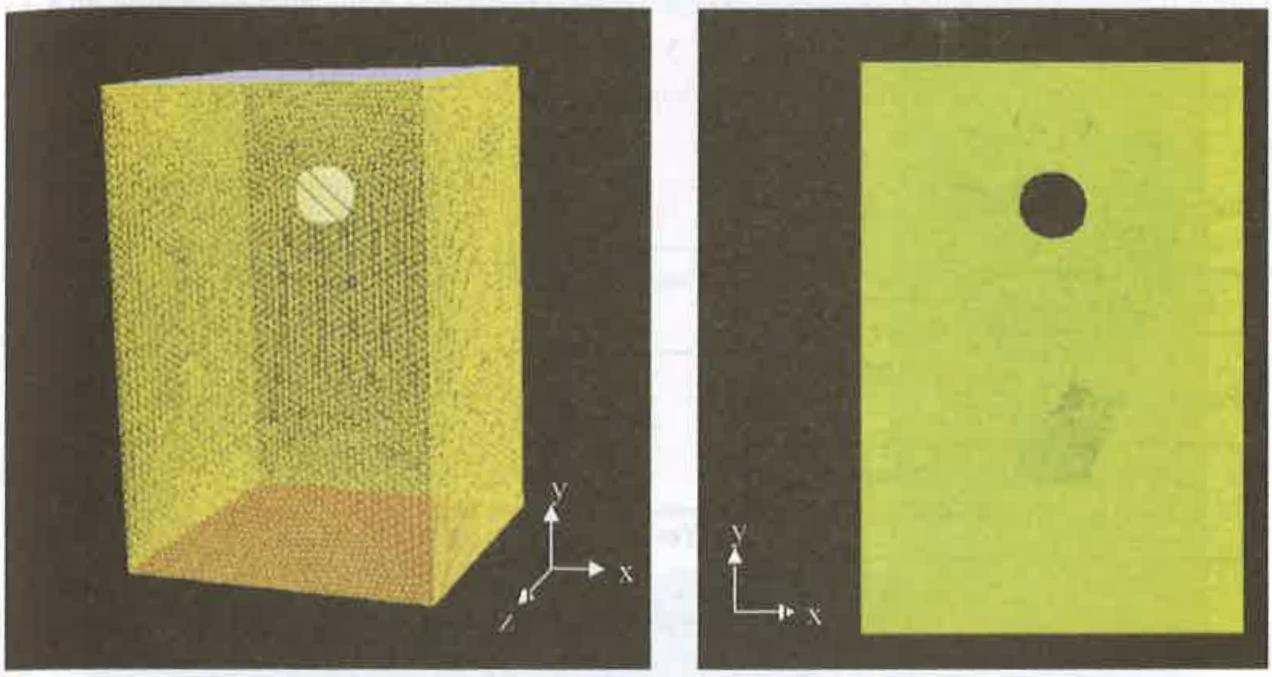

3-D Computational Model 2-D Centre Plane

Figure 2: 3-D computational model of the cricket ball

A triangular control volume mesh comprised of 2,274,270 nodes was generated on the computational model for facilitating the solution of flow transport equations. The resolution of the mesh was varied throughout the domain for optimizing the accuracy of the solution and to compromise with the computational time and cost.

Ansys Fluent 6.3.26, a commercial CFD tool has been used for the modelling process during which the transport equations are discretized to solve them numerically. The governing equations were solved by using Large Eddy simulation approach. The standard k-ε model was used for modelling turbulence. Turbulent intensity and turbulent length scale approach was utilized for initiating turbulence calculations during the simulations. It was observed that the roughness height of the surface of a new cricket ball varies from one location to another. The value used by Sayers (2001) in his experiments was 0.3 mm and hence it was applied for the present simulations as well. Boundary conditions applied for the model are shown in Table 1.

Table 1: Boundary Conditions

Physical Geometry	Boundary Conditions
Inlet (Top Surface)	Velocity-Inlet
Outlet (Bottom Surface)	Pressure-Outlet
Open Boundaries	Symmetry
Cricket Ball	Non-rotating Wall

Figure 3 illustrates the modelling process adopted during this study. Simulations were run on a 3.2 GHz workstation of 4.0 GB RAM at the Faculty of Engineering of General Sir John Kotelawala Defence University, Sri Lanka until convergence took place as shown in Figure 4.

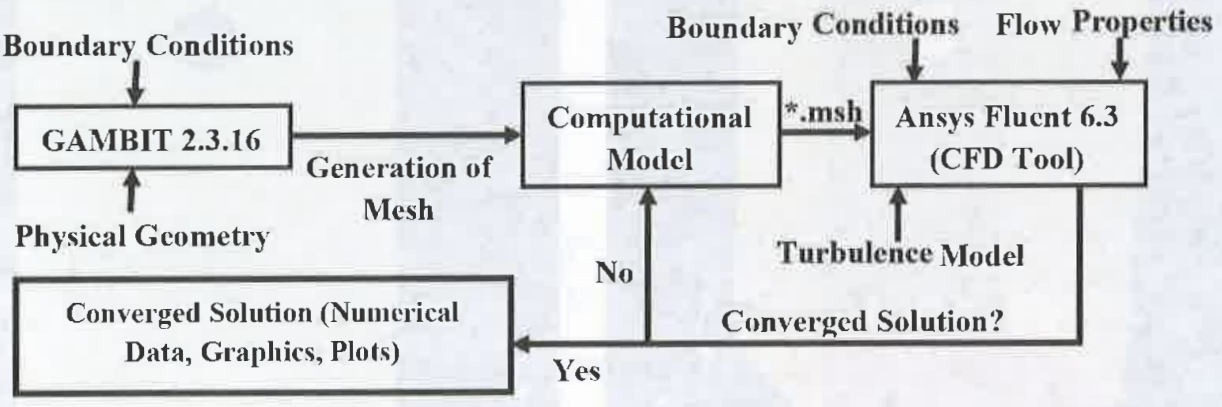

Figure 3: Modelling Process

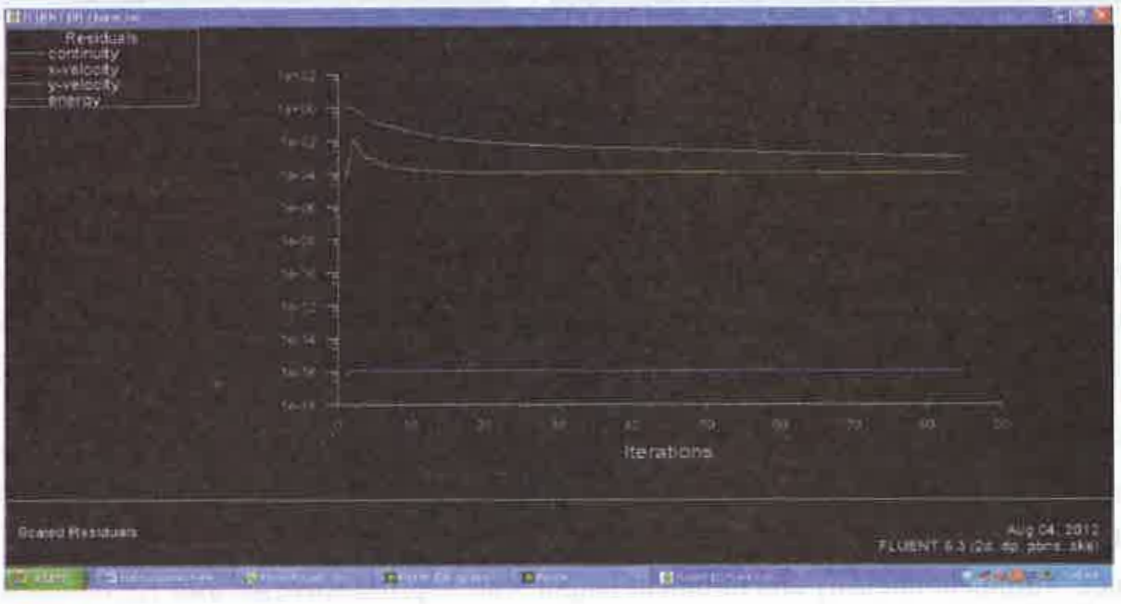

Figure 4: Simulation iterations reaching convergence

4. Results and Discussion

4.1 Total Pressure Distribution for varying Seam Angles

CFD simulations were performed until a converged solution was generated for each scenario. Some of the important predicted profiles generated by the simulations are interpreted in this section. Figure 5 shows predicted total pressure profiles in the computational domain when the seam angle is 0^0.

Figure 5: Total Predicted Pressure for seam angle 0^0

It is seen from the predicted pressure profiles that the aerodynamic forces on both smooth and rough sides of the cricket ball are almost identical due to the symmetrical nature of the flow regime over the ball. Therefore for this orientation of the seam a noticeable resultant side force on the ball is not generated and hence the conventional swing is not possible irrespective of the speed of delivery.

Further CFD simulations were run using geometrical models with the seam placed at an angle to the line of delivery of the ball. Figures 6 and 7 illustrate the variation of total predicted pressure in the computational domain when the resultant side force on the cricket ball is at a maximum level enabling optimum conventional swing at seam angles 30^0 and 45^0 respectively.

Figure 6: Total Predicted Pressure at seam angle 30^0 for optimum conventional swing

When the seam angle is 30^0, optimum conventional swing is predicted to take place at a delivery speed of 112 kmh^{-1} and the corresponding side force for the scenario is 0.64 N, which accounts for nearly 40% of the weight of the ball.

Figure 7: Total Predicted Pressure at seam angle 45^0 for optimum conventional swing

It is estimated that when the seam angle is 45^0, optimum conventional swing takes place at a delivery speed of 106 kmh^{-1} and the corresponding side force is 0.55 N.

4.2 Turbulent Intensity for varying Seam Angles

Figure 8 shows the predicted turbulent intensity profiles when the seam angle is 0^0.

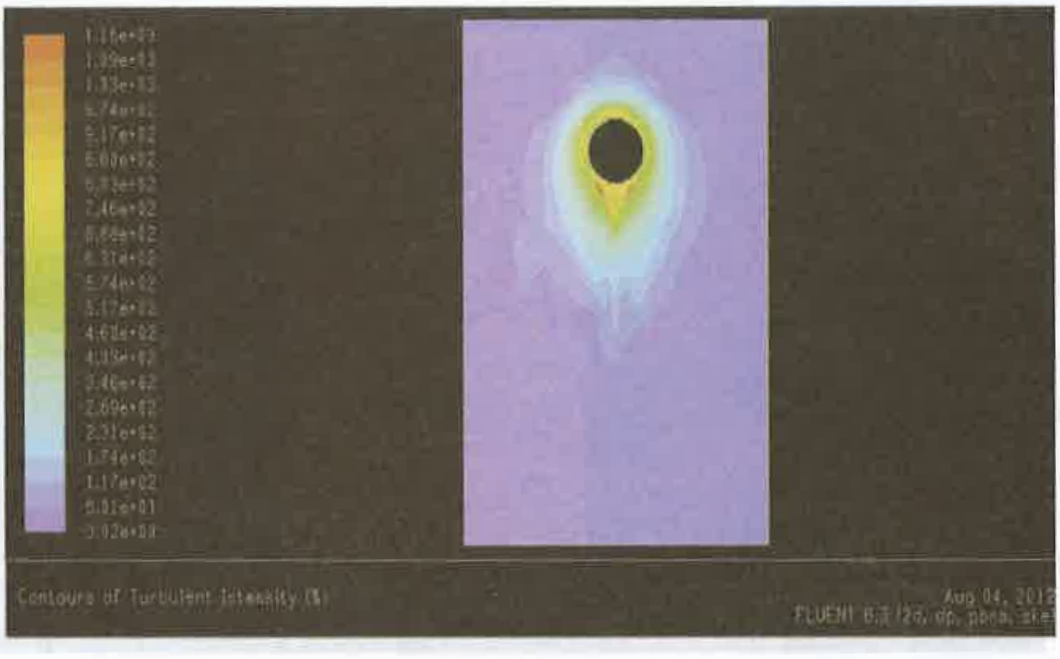

Figure 8: Predicted Turbulent Intensity for seam angle 0^0

Through the predicted turbulent intensity profiles it is observed that the flow over both the smooth and rough sides of the cricket ball has identical flow characteristics. Hence conventional swing caused by the pressure reduction on a particular side is not possible in this case. Figures 9 and 10 illustrate the variation of predicted turbulent intensity in the computational domain when optimum conventional swing of the ball takes place at seam angles 30^0 and 45^0 respectively.

Figure 9: Predicted Turbulent Intensity at seam angle 30^0 for optimum conventional swing

Figure 10: Predicted Turbulent Intensity at seam angle 45^0 for optimum conventional swing

It is observed from the predictions that during optimum conventional swing, shiny side of the ball experiences laminar flow and the rough side is subjected to turbulent flow. Flow over the rough side becomes turbulent due to the disruption of flow caused by the seam. Turbulent flow gets separated from the rough surface of the ball late, reducing pressure on that side. The difference in pressure between the two sides of the ball will make the ball move towards the rough side due to the resultant side force on the ball. Hence the ball will move in the direction of the seam causing conventional swing. It is clear from Figure 9 that when the seam angle is 30^0, flow on the rough side becomes more turbulent and the pressure difference between the two sides of the ball becomes more. Hence it will experience more conventional swing under the said condition.

4.3 Magnitude of Aerodynamic Side Force for varying Delivery Speeds

According to the present analysis optimum conventional swing can be achieved when the ball is delivered at 112 kmh^{-1} with a 30^0 seam angle. In this case the resultant side force on the ball is approximately 40% of the weight of the ball. If the ball is pitched at good length (approximately 6-8 m from batting crease) under the aforementioned conditions, the total deviation of the ball from the line of delivery during its flight is predicted to be approximately 25 cm. At speeds higher than 112 kmh^{-1}, the side force will reduce drastically and at speeds beyond 130 kmh^{-1} it is difficult to achieve conventional swing as shown in Figure 11.

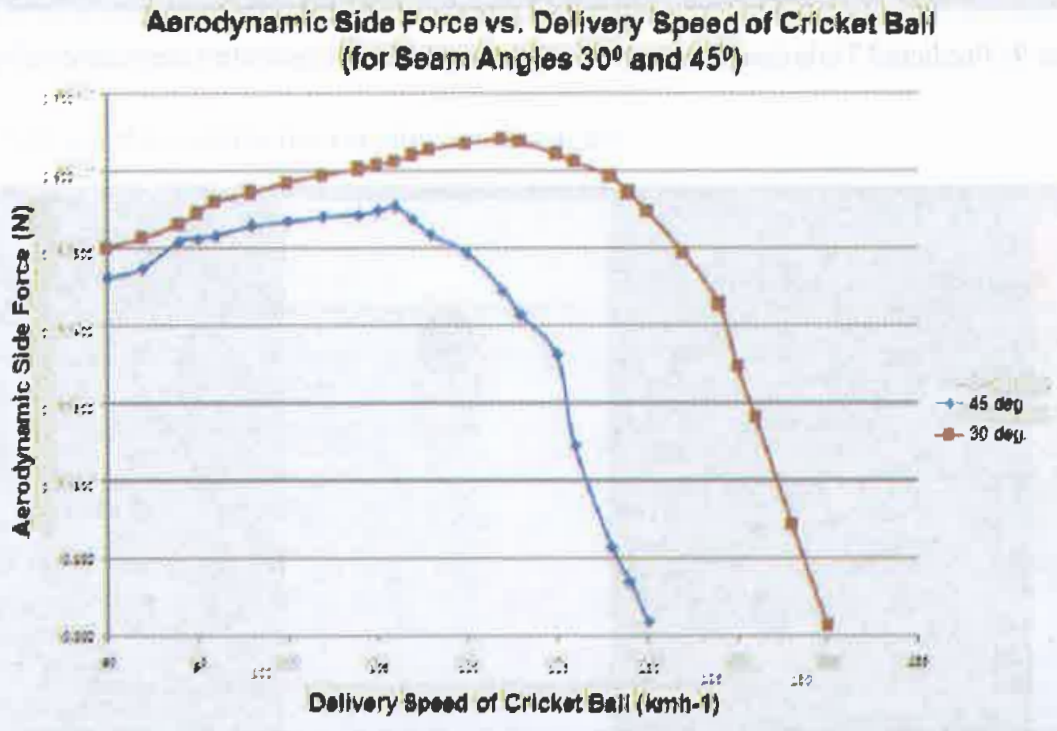

Figure 11: Variation of aerodynamic side force with the delivery speed of cricket ball

This prediction was further supported by the turbulent intensity profiles generated in the vicinity of the cricket ball. Conventional swing can be optimized at lower speeds by having a larger seam angle. This was evident as the delivery speed for the case of optimum swing for 45^0 seam angle is only 106 kmh^{-1} but with a lower side force.

5. Conclusion

The study is confined to the analysis of conventional swing undergone by a non-spinning cricket ball and the primary variables involved are the speed of delivery and seam angle. Modelling actual flow problems using CFD tools has been a challenge due to many reasons. Generating the mesh over the geometry and the computational domain was a tedious task. Representation of the physical geometry, flow properties and turbulent characteristi cs of the actual flow problem in the computational model was done with utmost care although this always involves certain unavoidable uncertainties. However the results are in reasonable agreement with the analysis of Mehta (1985). The main drawback of this study is the absence of measured data for validating the primary variables and the model. However, with the availability of a wind tunnel facility with smoke injection mechanisms for flow visualization, more accurate predictions through a refined computational model will be possible.

References

Barton, N. G. (1982) On the Swing of a Cricket Ball in Flight. *Proceedings of the Royal Society of London – Series A,* 379, pp. 109 – 131.

Bentley, K., Varty, P., Proudlove, M. and Mehta, R. D. (1982) An Experimental Study of Cricket Ball Swing. *Aero Tech. Note*, Imperial College, London, England, pp. 82-106.

Launder, B. E. and Spalding, D. B. (1974) The Numerical Computation of Turbulent Flows. *Computer Methods in Applied Mechanics and Engineering,* vol. 3, pp. 269-289.

Mehta, R. D. (1985) Aerodynamics of Sports Balls. *Annual Reviews Fluid Mechanics,* vol. 17, pp. 151-189.

Sayers, A. T. (2001) On the Reverse Swing of a Cricket Ball – Modelling and Measurements. *Proceedings of the Institution of Mechanical Engineers – Part C,* vol. 215, pp. 45-55.

Sayers, A. T. and Hill, A. (1999) Aerodynamics of a Cricket Ball. *Journal of Wind Engineering and Industrial Aerodynamics,* vol. 79, pp. 169-182.

Sayers, A. T. and Lelimo, N. J. (2007) Aerodynamic Coefficients of Stationary and Spinning Cricket Balls. *R & D Journal of the South African Institution of Mechanical Engineering,* 23(2).

Sherwin, K and Sproston, J. L. (1982) Aerodynamic of a Cricket Ball. *International Journal of Mechanical Engineering Education,* vol. 10, pp. 71-79.